Surface Micro-Structuring of Silica Glass by Laser-Induced Backside Wet Etching with ns-Pulsed UV Laser at a High Repetition Rate

Hiroyuki Niino, Yoshizo Kawaguchi, Tadatake Sato, Aiko Narazaki, Thomas Gumpenberger, and Ryozo Kurosaki

Photonics Research Institute,
National Institute of Advanced Industrial Science and Technology (AIST),
Tsukuba Central 5, 1-1-1 Higashi, Tsukuba, Ibaraki 305-8565, Japan
niino.hiro@aist.go.jp

Surface micro-structuring of silica glass plates was performed by using laser-induced backside wet etching (LIBWE) upon irradiation with a single-mode laser beam from a diode-pumped solid-state UV laser at 266 nm. We have succeeded in a well-defined micro-pattern formation without debris and microcrack formations around the etched area on the basis of galvanometer-based point scanning system with the laser beam. The behavior of liquid ablation (explosive vaporization) was monitored by impulse pressure detection with a fast-response piezoelectric pressure gauge. LIBWE method is suitable for rapid prototyping and rapid manufacturing of surface microstructuing of silica glass as mask-less exposure system in a conventional atmospheric environment.

Keywords: laser ablation, explosive vaporization of liquid, diode-pumped solid state UV laser, single mode laser beam, silica glass, surface micro-structuring

1. Introduction

Laser-induced micro-structuring of various materials has served as an important technique in surface fabrication for optics and optoelectronic devices [1]. In particular, significant attention has been given towards the micro-structuring of silica glass in spite of the difficulty involved, since silica is a commonly used material. The use of pulsed lasers can involve several approaches, such as conventional UV laser ablation [2], vacuum UV laser processing [3,4], pulsed-laser-generated x-ray [5], plasma-assisted UV ablation [6,7], and femtosecond laser micromachining [2,8]. We have demonstrated a novel one-step method, laser-induced backside wet etching (LIBWE), for micro- fabrication on a silica glass plate, involving irradiation with nanosecond-pulsed UV lasers [9-36]. The LIBWE method is based on the deposition of laser energy onto a thin layer at the glass-liquid interface during the explosive vaporization (ablation) of a liquid substance. Assuming negligible UV absorption by the silica glass, the incident laser beam passes through the glass plate resulting in the excitation of the dye solution. When the dye solution close to the interface becomes ablated using laser irradiation with sufficient fluence, etching on a surface layer of the silica glass is achieved. The depth of the etch increases linearly with the number of laser shots. Typical etch rates of the material were 0.1–40 nm pulse^{-1}, depending on irradiation conditions such as laser wavelength, laser fluence, and dye concentrations.

Micro-fabrications of various transparent materials, such as silica glass [9,12-16,18-27,29,30,34, 35], quartz [10,25,28, 31-33], glasses (Pyrex, etc.) [26], calcium fluoride [12,25,32], magnesium fluoride [25], barium fluoride [32], fluorocarbon resin [11], and sapphire [17,25,32,36], have been reported. Furthermore, various dye solutions, such as pyrene/acetone [9,10,12,13,17,18,19,24-27,31-33], pyrene/tetrahydrofuran (THF) [11,33], pyrene/ tetrachloroethylene [25,26,28,29], pyrene/cyclohexane [25], pyrene/toluene [26-30], pyranine/water [14], naphthalenesulfonic acid/water [15,20,22], naphthalene/methyl methacrylate [34,35], phenolphthalein/N-methyl-2-pyrrolidone [36], and pure toluene [16,21,22,23], have been used in conjunction with irradiation with KrF, XeCl, ArF and XeF excimer lasers. The micro-fabrication is applicable into random-phase-plates [31], Fresnel lens [32], beam-homogenizers (plano-convex microlens array) [33], surface relief gratings [26], imprinting templates [20], and microarrays of dye, protein, and polymer-microbeads [18,19]. By the analyses of time-resolved shadowgraph imaging [15,16,22] and transient pressure measurement [21,23], the dynamics of liquid vaporization was monitored to estimate the initial pressure and propagation rate of vapor bubbles.

In this paper, we report on the fabrication of various fine patterns on silica glass using the LIBWE method upon laser irradiation with a galvanometer-based point scanning system of a single-mode laser beam from a diode-pumped solid state (DPSS) laser at 266 nm. As the laser beam is scanned on the sample surface with the galvanometer controlled by a computer for flexible operations, galvanometer-based point scanning system is suitable for a rapid prototyping process according to electronic design data in the computer.

2. Experimental

2.1 Galvanometer-based point scanning system with a single-mode DPSS UV laser

An Nd:YVO$_4$ laser at the fourth harmonic wavelength (λ= 266 nm, FWHM 30 ns, M^2< 1.3) was used as a light source in ambient condition. The laser was used at the repetition rate of 10-20 kHz. The laser beam with a Gaussian beam profile in intensity was scanned with galvanometer-based point scanning module (GSI Lumonics,

HPM10M2). Optics of a zoom-beam-expander (Sill Optics), pinhole, and telecentric scan lens (Sill Optics, focus length: 100 mm) were used to obtain a scanning laser beam with a small focused spot size, as shown in Fig. 1. A fused-silica glass plate (Tosoh SGM Co., ES grade) with a thickness of about 2 mm was used as a sample. The glass sample was mounted on a stage. Toluene (Wako Pure Chemical Industries Ltd., S grade) was used without further purification. The penetration depth (d) of pure toluene solution at the wavelength of 266 nm was estimated to be 6.1 μm on the basis of single photon absorption ($d=Mw/\varepsilon\rho$; $Mw= 92$ g mol^{-1}, $\rho= 0.86$ kg dm^{-3}, $\varepsilon= 175$ mol^{-1} dm^3 cm^{-1} (hexane solution) [37]). The morphology of etched patterns was analyzed using a confocal scanning laser microscope (Keyence, VK-8500) and scanning electron microscope (Keyence, VE-7800).

In addition, replication process was performed by silicone elastomer resin. A fluid oligomer (Dow Corning Co., Sylgard 184) mixed with a small portion of a thermo-crosslinker was cast on the glass template, and croslinkage was performed at the temperature of 350 K.

2.2 Transient pressure measurement of toluene vaporization

Transient pressure caused by laser vaporization of toluene liquid was directly measured with a fast-response piezoelectric pressure gauge (Dr. Müller Ingenieurtechnik, Müller-Platte-Gauge, Germany) specifically designed for increased tolerance for use in toluene [23]. The distance between the sensor and glass surface was set at 0.5 mm. The signals were recorded by a digital oscilloscope that allows fast digitizing of long-duration events (LeCroy 9310AL).
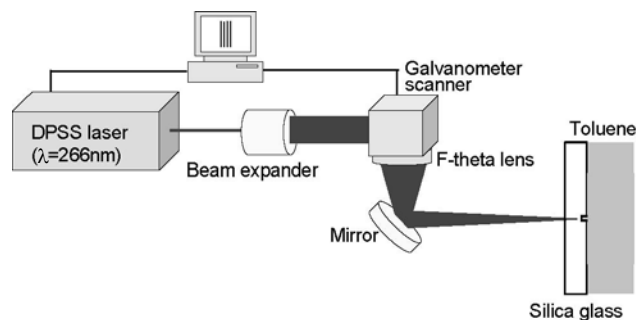

Fig. 1 Experimental setup for the LIBWE by using Galvanometer-based point scanning system.

3. Results and Discussion
3.1 Microstructuring of silica glass with galvanometer scanning system

Well-defined etching grooves with ca.15 μm in width, which was free of debris and microcracks around the area, were fabricated by UV laser irradiation using a single-mode laser beam, as shown in Figs. 2-6. The laser irradiation was carried out at laser power of 10 μJ pulse^{-1} with the repetition rate of 10 kHz. The laser beam was scanned on the sample surface at the rate of 100 mm s^{-1}. Upon the scanning irradiation accumulated up to twenty scans at the same positions to make a deep groove structure on the surface, the etch depth was increased as increase with the number of scanning times. The replica of the

etched groove indicated a Gaussian shape due to the intensity profile of the incident laser beam (Figs. 4 and 6).
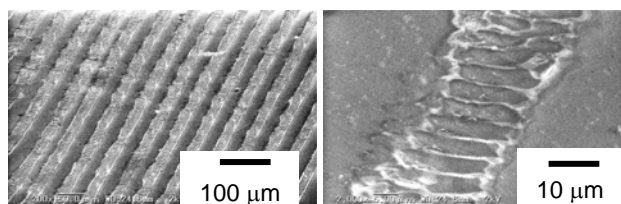

Fig. 2 SEM pictures of silica glass structured by LIBWE upon the laser irradiation with a single scan at 10 kHz and 10μJ pulse^{-1} (beam scan rate: 100 mm s^{-1}).
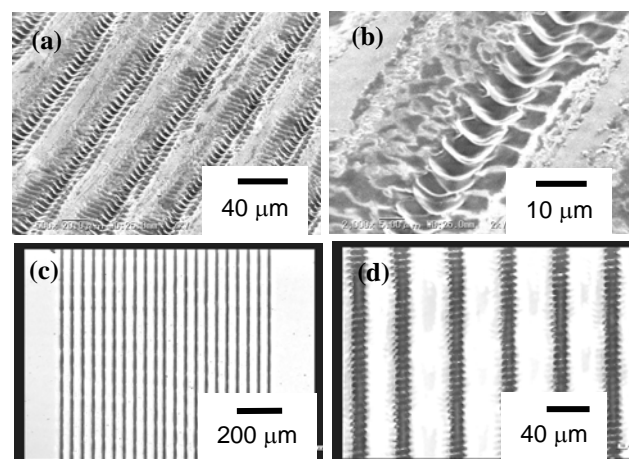

Fig. 3 SEM (a,b) and optical (c,d) pictures of silica glass structured by LIBWE upon the laser irradiation with ten-times scans at 10 kHz and 10μJ pulse^{-1} (beam scan rate: 100 mm s^{-1}).
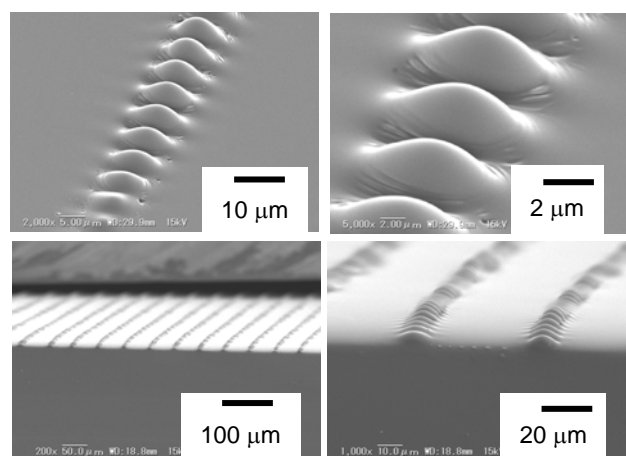

Fig. 4 SEM pictures for the replica surface from the glass of Figure 3. Each picture has a different magnification.

On the other hand, when a tightly focused beam of the single-mode UV laser was incident without liquid in the air, well-defined etching pit with 10 μm in diameter was formed on the silica glass by a conventional ablation, as shown in Fig. 7(a,b) [38]. However, upon the irradiation of several laser shots accumulated at the same position to make a deep pit structure on the surface, cracks were randomly formed around etched area (Figs. 7(c,d)), indicating that single-shot irradiation was a key for this well-defined micro-fabrication at the conventional ablation condition. As LIBWE process enables one to accumulate laser pulses at the same position for making a deep hole on the surface without crack formation, the use of LIBWE allows great flexibility in the types of processing and the geometries of the structures such as micro-channels, grating and deep pits.

As the laser beam is scanned on the sample surface with the galvanometer according to the pattern produced with a computer, a centimeter-sized component structured by a line-patterned grating was easily fabricated on a silica glass plate by laser beam scanning (Fig. 8). It is demonstrated that galvanometer-based point scanning system is suitable for a flexible rapid prototyping without a mask projection.
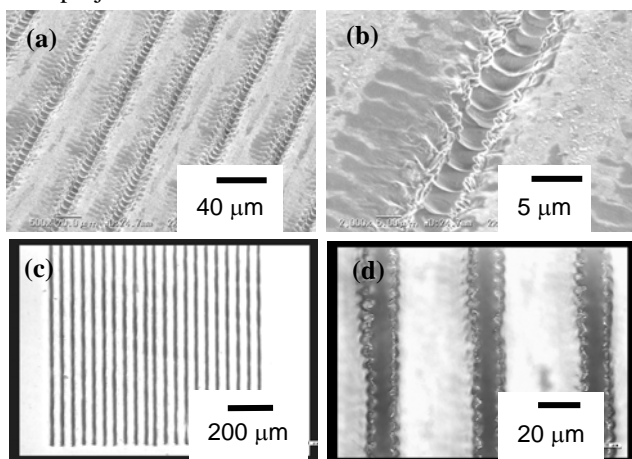

Fig. 5 SEM (a,b) and optical (c,d) pictures of silica glass structured by LIBWE upon the laser irradiation with twenty-times scans at 10 kHz and 10μJ pulse^{-1} (beam scan rate: 100 mm s^{-1}).
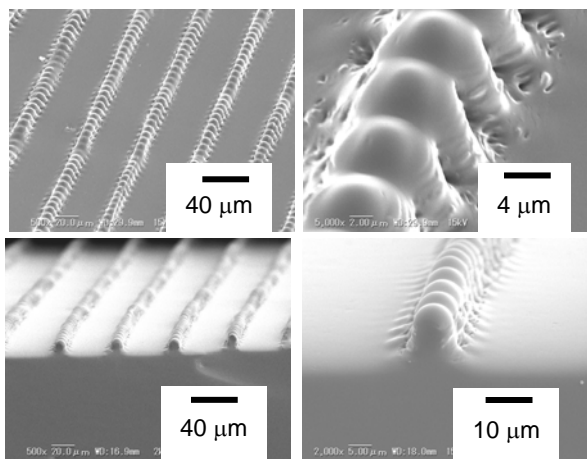

Fig. 6 SEM pictures for the replica surface from the glass of Figure 5. Each picture has a different magnification.
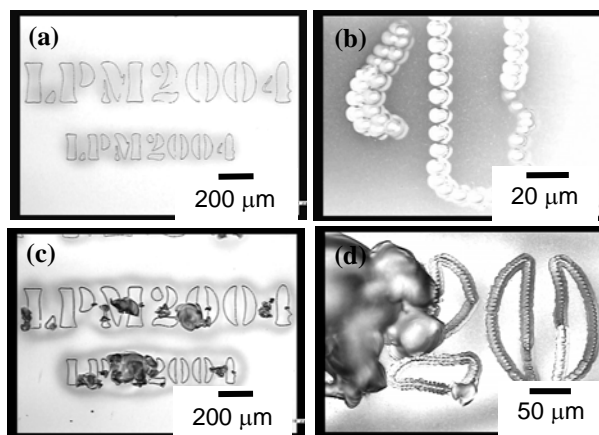

Fig. 7 Optical micrographs of silica glass surface after conventional laser ablation in the air; (a,b) single scan of laser beam, (c,d) twice scans of laser beam.
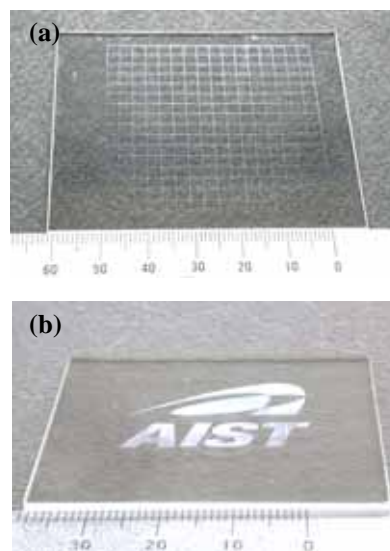

Fig. 8 Optical pictures of silica glass structured by LIBWE; (a) square grid array, (b) AIST-logotype of a line-patterned grating. Scale is 1 mm/division.

3.2 Transient pressure measurement of toluene vaporization

According to optical images monitored by time-resolved shadowgraph technique, the laser vaporization of toluene liquid showed shockwave propagation and vapor expansion at the interface between silica glass and toluene liquid [16,22,23]. These transient phenomena were induced by the explosive vaporization of the liquid. In the present study by DPSS UV laser irradiation at a high repetition rate, the vapor formation might be adversely affected because the period for the expansion and contraction of a vapor bubble was in the order of microsecond. Figure 9(a) shows a transient pressure profile during the DPSS laser irradiation with fluence of 520 mJ cm^{-2} at 10 Hz (laser spot: 50 μmφ). A pair of impulses corresponded to shock wave formation by vapor expansion (bubble formation in toluene vaporization) and collapsing was clearly observed [23]. The time duration of the pair is ca. 45 μs. In Figs. 9(b) and 9(c) of pressure profile at 5 kHz and 10 kHz, respectively, the pairs of

impulses were steadily monitored. The intensity of the pressure signals was not stable in Figure 9 (b) and (c) whereas the incident lasers energy was constant. This was probably due to instability of liquid expansion and collapsing.
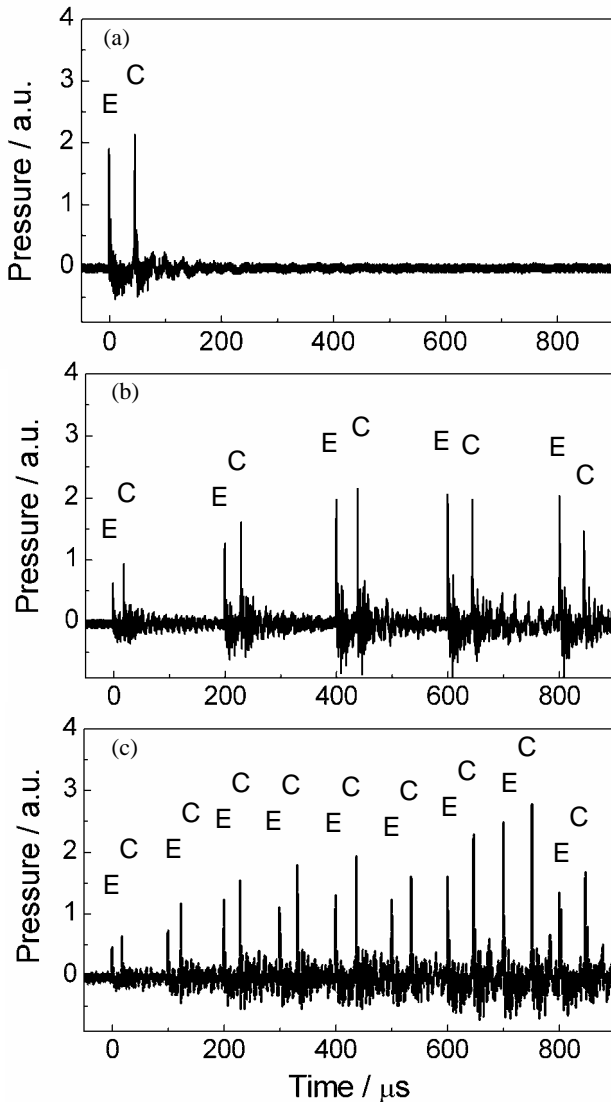

Fig. 9 Transient pressure signals caused by toluene explosive vaporization by DPSS laser at 0.52 J cm^{-2} and 50 μmφ; (a) repetition rate of 10 Hz, (b) 5 kHz, (c) 10 kHz. Signal impulses marked with "E" are due to vapor expansion and those with "C" are due to collapse of the bubble.

When the repetition rate of the laser irradiation increased up to 20 kHz, the pairs of impulses were able to detect clearly. Figure 10 shows the pairs of impulses formed by the first four laser shots at a fluence of 5.7 J cm^{-2} and laser spot of 12 μmφ. The pairs of the signals were also observed distinctly in the total irradiation period expanded to 15 ms, in which 300 laser shots were involved. All of the pressure signals in 15 ms are illustrated as a three-dimensional mapping in Fig. 11, where Y axis of time proceeds from top to bottom and X axis is the series of laser shots at 20 kHz. Time in Figure 11 starts at the same time as each laser irradiation pulse coming to the target.

Black-colored spots in the figure correspond to an impulse of pressure signals caused by bubble expansion and collapsing. The time duration of the pairs in the whole time region is dominantly observed in the range of 25-35 μs. The observation suggests that LIBWE is possible by the DPSS UV laser irradiation at a high repetition rate of several tens kHz.
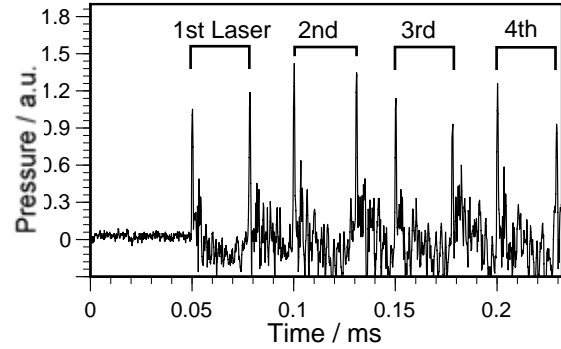

Fig. 10 Transient pressure profile of toluene ablation by DPSS UV laser irradiation at repetition rate of 20 kHz (fluence: 5.7 J cm^{-2}, laser spot: 12 μmφ).
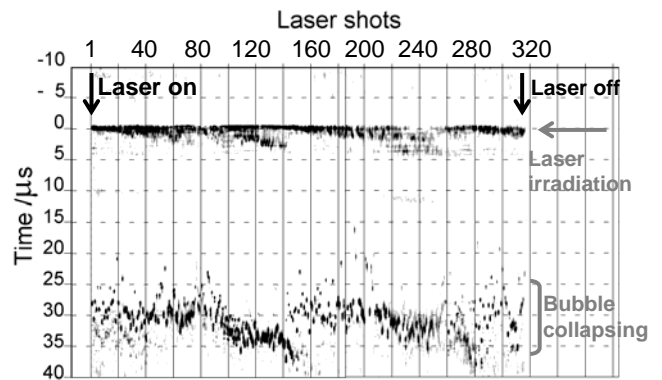

Fig. 11 Three-dimensional mapping of pressure signal of toluene ablation in the period of 15 ms by DPSS UV laser irradiation with the condition same as Figure 10 (repetition rate: 20 kHz). Black spots correspond to an impulse of pressure signals.

4. Summary

We have demonstrated that well-defined micropattern on a silica glass plate was fabricated by LIBWE method using galvanometer-based point scanning of DPSS UV laser. The point scanning system on a high repetition rate is suitable for a flexible rapid prototyping as mask-less exposure system. For precise patterning with a high resolution, on the other hand, mask projection system with an excimer laser has an advantage. Both the systems would be complementally utilized in mass production. Although transient shockwaves and micro-bubbles induced by laser ablation of the liquid expanded to the surroundings in the nano- and micro-second timescale upon the laser irradiation at a repetition rate of 10 kHz, the well-defined micro-fabrications were successfully performed on the glass surfaces without any crack or debris formation.

References

[1] D. Bäuerle, Laser Processing and Chemistry, 3rd Edn., Springer, Berlin, Heidelberg, (2000).

[2] J. Ihlemann, B. Wolff, P. Simon, Appl. Phys., **A54**, (1992) 363.

[3] P. R. Herman, R. S. Marjoribanks, A. Oettl, K. Chen, I. Konovalov, S. Ness, Appl. Surf. Sci., **154–155**, (2000) 577.

[4] K. Sugioka, S. Wada, H. Tashiro, K. Toyoda, A. Nakamura, Appl. Phys. Lett., **65**, (1994) 1510.

[5] T. Makimura, H. Miyamoto, Y. Kenmotsu, K. Murakami, H. Niino, Appl. Phys. Lett., **86**, (2005) 103111.

[6] J. Zhang, K. Sugioka, and K. Midorikawa, Opt. Lett., **23**, (1998) 1486.

[7] J. Zhang, K. Sugioka, and K. Midorikawa, Appl. Phys., **A67**, (1998) 499.

[8] H. Varel, D. Ashkenasi, A. Rosenfeld, M. Wähmer, E. E. B. Campbell, Appl. Phys., **A65**, (1997) 367.

[9] J. Wang, H. Niino, A. Yabe, Appl. Phys., **A68**, (1999) 111.

[10] J. Wang, H. Niino, A. Yabe, Appl. Phys., **A69**, (1999) S271.

[11] J. Wang, H. Niino, A. Yabe, Jpn. J. Appl. Phys., **38**, (1999) L761

[12] J. Wang, H. Niino, A. Yabe, Appl. Surf. Sci., **154-155**, (2000) 571.

[13] Y. Yasui, H. Niino, Y. Kawaguchi, A. Yabe, Appl. Surf. Sci., **186**, (2002) 552.

[14] X. Ding, Y. Yasui, H. Niino, Y. Kawaguchi, A. Yabe, Appl. Phys., **A75**, (2002) 437.

[15] X. Ding, Y. Kawaguchi, H. Niino, A. Yabe, Appl. Phys., **A75**, (2002) 641.

[16] H. Niino, Y. Yasui, X. Ding, A. Narazaki, T. Sato, Y. Kawaguchi, A. Yabe, J. Photochem. Photobiol. A: Chem., **158**, (2003) 179.

[17] X. Ding, T. Sato, Y. Kawaguchi, H. Niino, Jpn. J. Appl. Phys., **42**, (2003) L176.

[18] X. Ding, Y. Kawaguchi, T. Sato, A. Narazaki, H. Niino, Chem. Commun., (2003) 2168.

[19] X.Ding, Y.Kawaguchi, T.Sato, A.Narazaki, H.Niino, Langmuir, **20**, (2004) 9769.

[20] H. Niino, X. Ding, R.Kurosaki, A. Narazaki, T. Sato, Y. Kawaguchi, Appl. Phys., **A79**, (2004) 827.

[21] Y. Kawaguchi, X. Ding, A. Narazaki, T. Sato, H. Niino, Appl. Phys., **A79**, (2004) 883

[22] X. Ding, Y. Kawaguchi, T. Sato, A. Narazaki, R. Kurosaki, H. Niino, J. Photochem. Photobiol. A: Chem., **166**, (2004) 129.

[23] Y. Kawaguchi, X. Ding, A. Narazaki, T. Sato, H. Niino, Appl. Phys., **A80**, (2005) 275.

[24] Y. Kawaguchi, T. Sato, A. Narazaki, R. Kurosaki, H. Niino, Jpn. J. Appl. Phys., **44**, (2005) L176.

[25] R. Böhme, A. Braun, K. Zimmer, Appl. Surf. Sci., **186**, (2002) 276.

[26] K. Zimmer, R. Böhme, A. Braun, B. Rauschenbach, F. Bigl, Appl. Phys., **A74**, (2002) 453.

[27] K. Zimmer, A Braun, R Böhme, Appl. Surf. Sci., **208-209**, (2003) 199.

[28] R. Böhme, D. Spemann, K. Zimmer, Thin Solid Films, **453-454**, (2004) 127.

[29] K. Zimmer, R. Böhme, Appl. Surf. Sci., **243**, (2005) 415.

[30] R. Böhme, J. Zajadacz, K. Zimmer, B. Rauschenbach, Appl. Phys., **A80**, (2005) 433.

[31] G. Kopitkovas, T. Lippert, C. David, A. Wokaun, J. Gobrecht, Microelectron. Eng., **67–68**, (2003) 438.

[32] G. Kopitkovas, T. Lippert, C. David, A.Wokaun, J. Gobrecht, Thin Solid Films, **453-454**, (2004) 31.

[33] G. Kopitkovas, T. Lippert, C. David, S. Canulescu, A. Wokaun, J. Gobrecht, , J. Photochem. Photobiol. A: Chem., **166**, (2004) 135.

[34] C. Vass, B. Hopp, T. Smausz, F. Ignacz, Thin Solid Films, **453-454**, (2004) 121.

[35] C. Vass, T. Smausz, B. Hopp, J. Phys. D: Appl. Phys., **37**, (2004) 2449.

[36] K. Fujito, T. Hashimoto, K. Samonji, J. S. Speck, S. Nakamura, J. Cryst. Growth **272**, (2004) 370.

[37] H.-H. Perkampus, "UV-vis Atlas of Organic Compounds", 2nd Edn., VCH, Weinheim (1992) p.338.

[38] H. Niino, Y. Kawaguchi, T. Sato, A. Narazaki, X. Ding, and R. Kurosaki, Proc. of SPIE, **5339**, (2004) 112.

[39] Y. Tsuboi, K. Hatanaka, H. Fukumura, H. Masuhara, J. Phys. Chem., **98**, (1994) 11237.